ELSEVIER

Journal of Crystal Growth 232 (2001) 376–386

JOURNAL OF CRYSTAL GROWTH

www.elsevier.com/locate/jcrysgro

Packing contacts in orthorhombic and monoclinic crystals of a thermophilic aspartyl-tRNA synthetase favor the hydrophobic regions of the protein

C. Charron, C. Sauter[1], D.W. Zhu[2], J.D. Ng[3], D. Kern, B. Lorber, R. Giegé*

Département 'Mécanismes et Macromolécules de la Synthèse Protéique et Cristallogenèse', UPR 9002, Institut de Biologie Moléculaire et Cellulaire du CNRS, 15 rue René Descartes, 67084 Strasbourg Cedex, France

Abstract

The thermostable aspartyl-tRNA synthetase (AspRS-1) from *Thermus thermophilus* is a 132 kDa homodimer with a subunit composed of 580 amino acids. It catalyses the aminoacylation of $tRNA^{Asp}$ with aspartic acid in the process of translating genetic information. Here we present data on crystals grown in the presence of two different crystallizing agents. A first crystal form (form A) grows in the presence of 0.8 M ammonium sulfate and exhibits the orthorhombic space group $P2_12_12_1$. Monoclinic plates (form B) grow in an aqueous solution of 6% (m/v) PEG-8000. In this study, the monoclinic crystal structure (form B) was solved by molecular replacement using the orthorhombic crystal structure as a model and refined to a 2.65 Å resolution limit. The contacts between molecules in both crystalline lattices are compared. Although the overall-accessible surface of the protein is more hydrophilic than average, the packing contacts in both lattices comprise mainly hydrophobic van der Waals interactions and only a few salt bridges and hydrogen bonds. Interaction areas are much larger in the orthorhombic than in the monoclinic lattice, and only 6 contact residues out of 134 are common.

PACS: 61.10.Nz ; 81.10.Dn ; 87.15.Kg

Keywords: A1. Crystal engineering; A1. Crystal packing; A1. Crystal structure; A1. X-ray diffraction; B1. Aspartyl-tRNA synthetase; B1. Proteins

1. Introduction

Genesis of crystals can be described from the point of view of either physics or chemistry. In the biomacromolecular field our understanding of crystal growth relies essentially on physics-based knowledge (e.g. [1–3]). However, proteins and other biomacromolecules have the natural potential to interact via hydrogen bonds, ionic, and Van der Waals contacts. Such contacts are precisely those occurring in intermolecular packing within macromolecular crystals. In an overall project of

*Corresponding author. Tel.: +00-33-3-88-41-70-58; fax: +00-33-3-88-60-22-18.

E-mail addresses: r.giege@ibmc.u-strasbg.fr (R. Giegé).

[1] Present address: EMBL Heidelberg, Meyerhofstrasse 1, 69012 Heidelberg, Germany.

[2] Present address: MRC Group in Molecular Endocrinology, CHUL Research Center and Laval University, Quebec, Canada G1 V 4G2.

[3] Present address: Laboratory for Structural Biology and the Department of Biological Sciences, The University of Alabama in Huntsville, Huntsville, AL 35899, USA.

0022-0248/01/$ - see front matter
PII: S0022-0248(01)01074-0

our laboratory we aim to understand how surface residues in a protein structure influence crystal growth, packing arrangement, and crystal quality. We intend also to investigate how engineering crystal surfaces modifies crystal properties. Our model protein is aspartyl-tRNA synthetase (AspRS-1) from *Thermus thermophilus* whose structure is known in an orthorhombic space group [4].

Here we present the first data on this chemistry-oriented crystallogenesis project. After justifying the choice of the model, we describe a novel monoclinic crystal form of *T. thermophilus* AspRS-1 and we compare it to the already known orthorhombic form obtained in the presence of a different crystallizing agent. X-ray data collection and structure determination of AspRS-1 in the monoclinic crystals are reported and particular attention is given to the comparison of the contacts between protein molecules in both crystalline lattices.

2. Materials and methods

2.1. Enzyme preparation and crystallization

The wild-type recombinant AspRS-1 from *T. thermophilus* was genetically over expressed in *Escherichia coli* and purified to homogeneity by a procedure described elsewhere [5]. Purity and activity were checked by SDS-PAGE and tRNA aminoacylation assays as described [6].

A sparse matrix was used to find crystallization conditions in solutions containing polyethylene glycol (PEG). Crystallizations were performed using the vapor diffusion method in hanging-drops [3,7]. Since crystal growth in gelled media may improve crystal quality [8], AspRS crystals were also prepared in 0.1% (m/v) agarose [9].

2.2. Crystallographic methods

X-ray diffraction intensity data were collected at the Deutsches Elektronen Synchrotron (DESY) at Hamburg (Germany) on the European Molecular Biology Laboratory (EMBL) beamline BW7B. The wavelength of the incident radiation was 0.8443 Å and the crystal-to-detector distance was 520 mm. Data were collected at cryogenic temperature using a Mar 34S IP detector. Prior to such data collection, a suitable native crystal was soaked in a cryobuffer composed of mother liquor containing 35% glycerol. The crystal was then flash-cooled in a nitrogen-gas stream at 100 K before mounting. Data were collected over a range of 218° with 1° oscillation per image and were processed using *DENZO* and *SCALPACK* [10].

The structure of AspRS-1 in the monoclinic space group was solved by molecular replacement with the program *AMoR*e [11] using the orthorhombic structure [4] as a template. Subsequent refinement was performed in the 30–2.65 Å range without non-crystallographic symmetry restraints using the *CNS* package [12]. Ten percent of the data were selected for R_{free} calculations and manual corrections of the model were performed using the program *O* [13].

The neighbors of an AspRS-1 molecule in a given crystal packing were generated using the program *O* [13]. Solvent-accessible surface areas were estimated with the algorithm by Lee and Richards [14] implemented in the *CNS* package [12]. The solvent probe radius was set at 1.4 Å. The surface area of a molecule buried by an intermolecular interaction is calculated as the difference between the accessible surface area of the molecule *in vacuo* and in the crystal. The cutoff distance was set at 4.5 Å for crystal contacts.

3. Results and discussion

3.1. Thermostable AspRS-1 as a model macromolecule

Aspartyl-tRNA synthetases belong to the aminoacyl-tRNA synthetase (aaRS) family which are the enzymes responsible for the attachment of amino acids to their cognate tRNAs in the process of translating genetic information [15]. These enzymes are partitioned into two families of 10 members each [16]. Catalytic mechanisms for the two-step aminoacylation reactions were proposed for class I [17] and class II aaRSs [18]. In the cytoplasm of most living cells, there is only one

aaRS for each of the 20 canonical amino acids. In some organisms, however, two aaRSs coexist for a same amino acid specificity. This is the case in the thermophilic eubacteria *T. thermophilus*, which contains two AspRSs, one of eubacterial type (AspRS-1) and one of archaeal type (AspRS-2) [19]. Here we consider AspRS-1 which is a class II enzyme charging aspartate on $tRNA^{Asp}$. This protein, like most class II aaRSs, is a homodimer with subunits related by a two-fold axis. It has a molecular weight of 132 kDa with a subunit composed of 580 amino acids and its crystal structure has first been determined at 2.5 Å resolution in the orthorhombic space group $P2_12_12_1$ [4]. The enzyme has a modular structure with a N-terminal domain recognizing the anticodon loop of tRNA which is connected to the active-site domain by a hinge region. This synthetase shows in addition a bulky extra domain specific to prokaryotic AspRSs which is inserted in the active-site domain.

Besides the biological importance of synthetases, several other reasons dictated the choice of AspRS-1 from *T. thermophilus* as a model protein for our crystallogenesis investigations. This enzyme is a representative of large oligomeric proteins by its irregular but well-defined shape (see Fig. 2). It distinguishes from more globular proteins or from proteins with flexible appended domains like the homologue AspRS from yeast [20]. Further, the protein is thermostable with a catalytic activity highest at 85°C [19]. Thermostability favors crystallizability and makes temperature variation experiments possible. Finally, orthorhombic crystals of AspRS-1 were already studied by physical [9,21] and chemical [22] approaches, and their quality was improved up to a diffraction limit of 2.0 Å at 20°C when crystallization was done in microgravity [23].

3.2. A novel crystal form of AspRS-1 growing in PEG solution

Crystals of proteins are usually grown from three main families of crystallizing agents (salts, organic solvents, or polymers of the PEG family [24,25]), but little is known about possible correlations between crystallization conditions, structural and chemical properties of proteins, and crystal features. Thus, with AspRS-1 from *T. thermophilus*, already known to yield orthorhombic crystals in the presence of ammonium sulfate (form A), we searched for a novel crystal form that would grow under markedly different solvent conditions. We chose PEG as the crystallizing agent with the aim to compare features of crystals of the same protein grown in the presence of ammonium sulfate and PEG.

After a sparse matrix search, and as expected, a novel crystal form of AspRS-1 growing in the presence of PEG-8000 (form B) was found. The crystals have the habit of monoclinic plates measuring up to 0.6 mm in length. They were also prepared in 0.1% (m/v) agarose gel under otherwise similar solution conditions, including PEG-8000. The correlation between growth conditions and crystal properties of these AspRS-1 crystals obtained in solution and in agarose gel is described elsewhere [9]. Fig. 1 displays typical crystals of both forms originating from the same batch of protein, first a representative orthorhombic crystal (form A) grown from an ammonium sulfate solution and second a monoclinic crystal (form B) grown in a gelified medium containing PEG. Optimal crystallization conditions and overall characteristics of each crystal form are summarized in Table 1.

In contrast to form A crystals grown from a salt solution which were stable enough to collect full data sets up to 2.0 Å resolution at room temperature [22], form B crystals obtained in PEG diffract at best to 2.5 Å and suffer from radiation damage. Thus, prior to data collection, they were soaked in a cryobuffer and flash-cooled before mounting. This allowed to collect a total of 199,684 reflections in the 30–2.65 Å resolution range at a synchrotron beamline. They were reduced to 45,185 unique reflections. The data set was 99.2% complete and R_{sym} was 7.6% on intensities ($R_{sym} = \Sigma|I - <I>|/\Sigma I$) (Table 2).

As with the orthorhombic crystals, monoclinic crystals of space group $P2_1$ have one dimer in the asymmetric unit (Table 1). Packing density ($V_m = 3.38\,Å^3\,Da^{-1}$) and solvent content (61.6%) are in good agreement with values known for other proteins [26]. For orthorhombic crystals (Table 1),

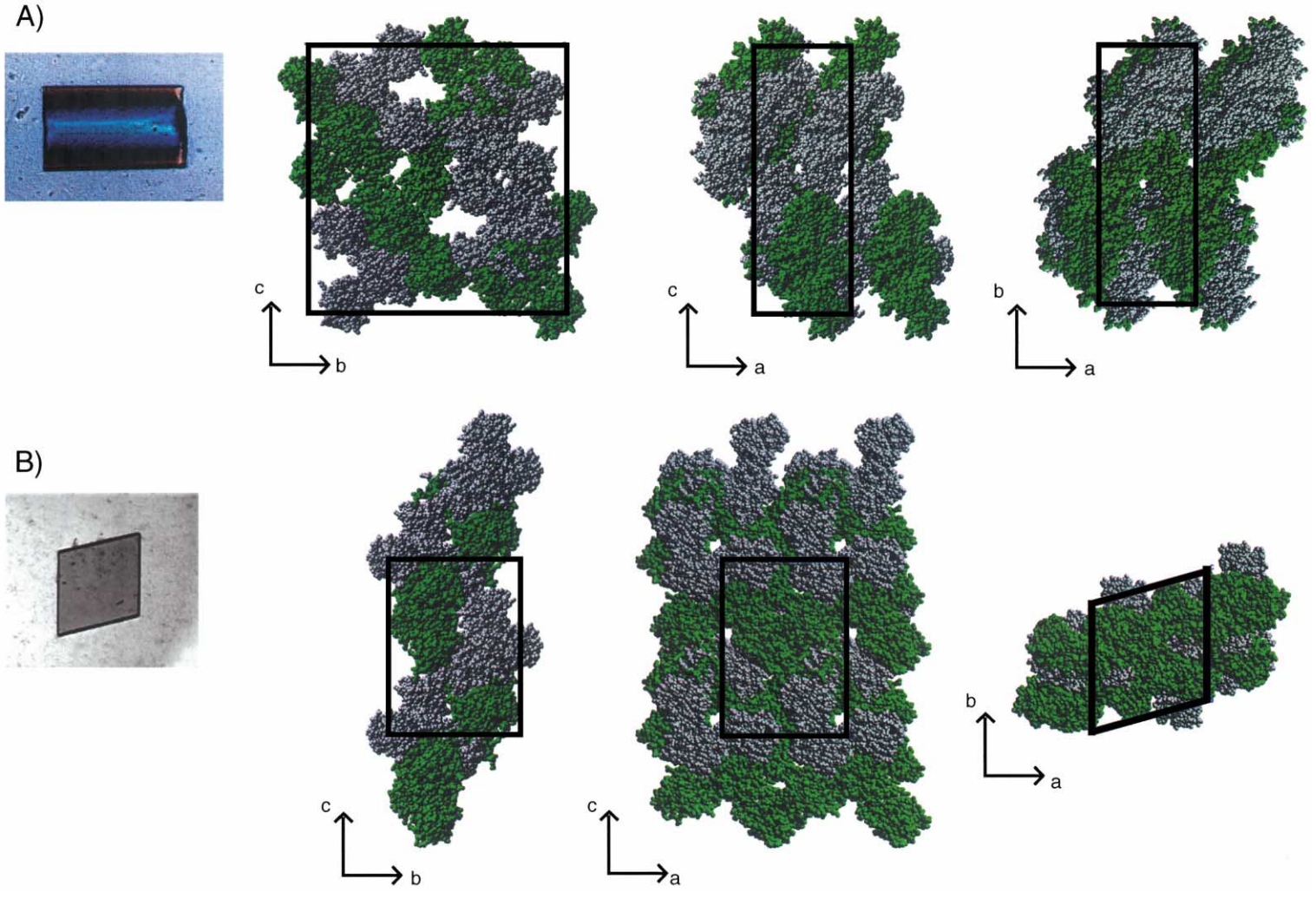

Fig. 1. Orthorhombic (A) and monoclinic (B) crystals of AspRS-1 and their packing within the orthorhombic (A) and monoclinic (B) crystalline lattices. The views of the crystals are at the same scale, with a size of ~ 0.6 mm in length for the monoclinic form in (B). The views of the unit cell contents are according to the three perpendicular orientations of the crystals. To facilitate interpretation of the packing arrangements, the subunits of AspRS-1 are colored differently in grey and green.

Table 1
Crystallization conditions and crystal data

Crystal type	Form A[a]	Form B[b]
Crystallization		
Protein concentration (mg/ml)	10	15
Crystallizing agent	Ammonium sulfate 0.8 M	PEG-8000 6% (m/v)
Buffer	Tris-HCl 25 mM pH 7.2	Tris-HCl 0.1 M pH 7.8 agarose 0.1% (m/v)
T(K)	293	293
Crystallization method	Dialysis (in microgravity)	Hanging drop
Crystal data		
Space group	$P2_12_12_1$	$P2_1$
Cell parameters (Å)	$a = 62.0$; $b = 156.1$; $c = 178.0$	$a = 83.2$; $b = 112.8$; $c = 88.0$ $\beta = 105.6^\circ$
Asymmetric unit content	One dimer	One dimer
V_m ($Å^3\,Da^{-1}$)	3.54	3.38
Solvent content (%)	64.4	61.6
Resolution limit (Å)	2.0	2.65
T(K)	293	100

[a] From Ng et al. [23].
[b] From Zhu et al. [9].

Table 2
X-ray data measurement statistics of monoclinic crystals (form B)

Resolution range (Å)	2.65–30
R_{sym} (overall) (%)	7.6
Completeness (overall) (%)	99.2
$\langle I/\sigma(I)\rangle$ (overall)	20.0
Multiplicity (overall)	4.4
R_{sym} (2.65–2.74 Å) (%)	15.9
Completeness (2.65–2.74 Å) (%)	98.8
$\langle I/\sigma(I)\rangle$ (2.65–2.74 Å)	8.1

respective values were $V_m = 3.54\,Å^3\,Da^{-1}$ and 64.4%.

3.3. Structure of AspRS-1 in monoclinic crystals

The monoclinic crystal structure was solved by molecular replacement in the resolution range 10–3.5 Å using the dimeric structure in the orthorhombic lattice as the probe. The rotation function calculated with a 69 Å integration radius had only two peaks with height of 16 r.m.s.d. The orientation corresponding to the first peak was used in the calculation of the translation function. It gave only one peak with a correlation of 55.4% and a R_{factor} of 41.1%.

To optimize the rotational and translational parameters of the dimer in the asymmetric unit, a rigid-body refinement was performed in the resolution range 30–4.0 Å. Each subunit was subdivided into three fragments (residues 1–278, 279–417, and 418–580) and each fragment was taken as an independent rigid body. As a result, the R_{factor} fell to 37.3%. The structure was then refined to the R_{factor} of 26.5% and R_{free} of 31.2%. Further refinement including the addition of solvent molecules (which could be important in additional packing contacts) is in progress (Charron et al., in preparation).

The structure of AspRS-1 from *T. thermophilus* in the monoclinic lattice is similar to that previously described in the orthorhombic lattice [4]. Like most class II aaRSs [27], it is a homodimer made of two subunits related by a two-fold axis. The contact area between subunits is 5570 $Å^2$ and this hidden surface is the same as in the structure solved in the orthorhombic space group [4]. The overall structure of each subunit consists of the four domains which were first visualized in the orthorhombic lattice (see above

and Fig. 2). The AspRS-1 monomers from monoclinic and orthorhombic crystals show a r.m.s.d. value of superimposed C^{α} positions of 0.80 Å (residues 1–565). However, the comparison of the two crystal structures reveals a significant displacement of the 15 C-terminal amino acid residues (566–580) with a r.m.s.d. value of superimposed C^{α} positions of 3.10 Å.

3.4. Packing of AspRS-1 in orthorhombic vs. monoclinic crystals

The packing of AspRS-1 in orthorhombic crystals is shown in Fig. 1A. Large channels 30 Å in diameter and smaller channels of ~10 Å in diameter run along the *a* axis and pass through the entire crystal. Other channels crossing the orthorhombic crystals are parallel to the *b* and *c* axis and are much smaller.

In monoclinic crystals (Fig. 1B), diameter of largest channels does not exceed 10 Å. They run parallel to the *a* and *b* axis. The channels parallel to the *b* axis cross the crystal through the ca plane which is formed by two consecutive layers of dimers related by the crystallographic 2_1 axis. Viewed over the bc plane, and especially over the ab plane, the packing of monoclinic crystals appears compact.

Altogether, the images displayed in Fig. 1 reveal a tighter arrangement of the AspRS-1 molecules in the monoclinic than in the orthorhombic lattice, in agreement with solvent content and V_m-values (Table 1).

3.5. Contact areas

The protein surfaces buried upon crystallization were calculated in both crystal forms (Tables 3 and 4) and are displayed in Fig. 2. In orthorhombic crystals (Fig. 2A), they are essentially located in the extra domain (area D) of AspRS-1 and in its central core (areas A and E). In monoclinic crystals (Fig. 2B), the situation is different with contact regions more scattered over the protein, especially in the extra domain of the synthetase (area D). Notice that the packing valence is 6 in orthorhombic crystals and 8 in monoclinic crystals. In other words, 3 types of contacts occurring twice are found in orthorhombic crystals (Table 3) and 4 types of contacts, also occurring twice, are present in monoclinic crystals (Table 4).

In the orthorhombic lattice (Table 3), 14.4% (7040 Å^2) of the total dimer-accessible surface is involved in crystal contacts. Half of the buried surface is observed between a dimer in position (x, y, z) and a dimer in position $(-x, -1/2+y, 1/2-z)$. This macrocontact takes 7.2% (3540 Å^2) of the total dimer-accessible surface. The contact surface between a dimer in position (x, y, z), and a dimer in position $(-1/2-x, 1-y, -1/2+z)$ is 4.2% and covers 2040 Å^2. Finally, contact surfaces are found between a dimer in position (x, y, z) and a dimer in position $(1+x, y, z)$. They correspond to 3% (1460 Å^2) of the total dimer-accessible surface.

It was shown that the crystal contact area per molecule increases with the compactness of the crystal [26]. Accordingly, for the more compact monoclinic AspRS-1 crystals (Tables 1 and 4), the total contact area should exceed that occurring in the orthorhombic packing. Surprisingly, however, only 7.8% (3840 Å^2) of the solvent-accessible surface of the dimer participate in intermolecular contacts, as compared to 14,4% in the orthorhombic lattice. The largest hidden surface occurs between a dimer in position (x, y, z) and a dimer in position $(-x, -1/2+y, -z)$. This macrocontact covers 3.7% (1800 Å^2) of the total solvent-accessible surface of the dimer. Another macrocontact exists between a dimer in position (x, y, z) and a dimer in positions $(-1+x, y, z)$ and represents 1.7% (820 Å^2). Further contacts are found between a dimer in position (x, y, z) and a dimer in position $(-x, -1/2+y, 1-z)$. They correspond to 1.6% (840 Å^2) of the total-accessible surface that is buried. Finally, a small contact region is found between a dimer in position (x, y, z) and a dimer in position $(-1-x, -1/2+y, -z)$ and corresponds to 0.8% (380 Å^2) of the total-accessible surface.

3.6. Nature of contact residues

Amino acids from AspRS-1 making intermolecular contacts in the orthorhombic and monoclinic lattices are listed in Tables 3 and 4. In both crystal lattices the contacts they generate are mostly of the

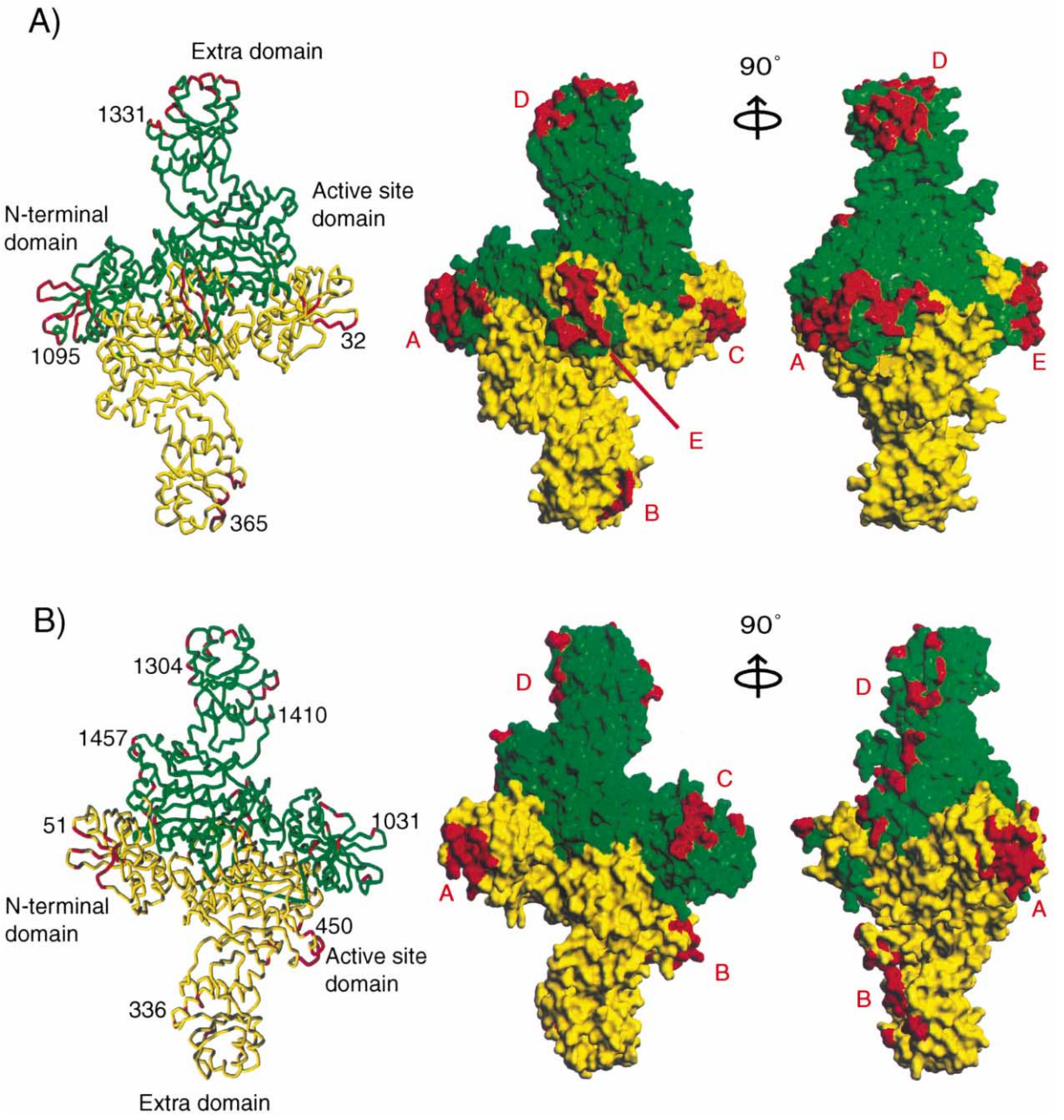

Fig. 2. Packing contacts between AspRS-1 molecules in orthorhombic (A) and monoclinic (B) crystals. Left views show the C-backbone of the dimer; central and right views are compact models of AspRS-1 emphasizing the solvent-accessible surface of the molecule. Numbering of amino acid residues starts in the first monomer in yellow (1–580) and continues through the second monomer in green (1001–1580); contact surfaces are colored in red. Notice that the synthetase is oriented differently (by a 180° rotation) in (A) and (B), so that to emphasize the faces of the protein where most of the contacts occur in each lattice (left and central views have the same orientation; right views are rotated by 90°).

Table 3
Molecular contacts in the orthorhombic packing

Contacts between dimers	Residues in interaction[a]			Buried surface[b]
$x, y, z \leftrightarrow -x, -1/2+y, 1/2-z$	R331 ↔ R1353^{i}	R1028 ↔ R64^{i}	D1030 ↔ T105^{vw}	$2 \times 1770\,\text{Å}^2$
$-x, 1/2+y, 1/2-z \leftrightarrow x, y, z$	G1032 ↔ K104^{vw}	R1064 ↔ R64^{i}	K1104 ↔ G32^{vw}	
	T1105 ↔ D30^{h}	S1330 ↔ A328^{vw}	K1327 ↔ S330^{vw}	
	A1328 ↔ R353^{vw}	S1330 ↔ K327^{vw}	R1331 ↔ E355^{i}	
	W1351 ↔ G361^{vw}	R1353 ↔ R1331^{i}	R1353 ↔ L1329^{vw}	
	R1353 ↔ E355^{i}	E1355 ↔ R353^{i}	S1360 ↔ S360^{h}	
	G1361 ↔ E355^{vw}	G1361 ↔ W1351^{vw}	G1383 ↔ R331^{vw}	
$x, y, z \leftrightarrow -1/2-x, 1-y, z-1/2$	G1016 ↔ K365^{vw}	E1018 ↔ K1365^{vw}	E1018 ↔ E1368^{vw}	$2 \times 1020\,\text{Å}^2$
$-1/2-x, 1-y, z+1/2 \leftrightarrow x, y, z$	L1034 ↔ V1049^{vw}	L1034 ↔ H1051^{vw}	P1052 ↔ G1033^{vw}	
	A1053 ↔ I1305^{vw}	A1053 ↔ A1373^{vw}	A1053 ↔ V1370^{vw}	
	P1055 ↔ E1372^{vw}	P1055 ↔ R1371^{vw}	P1055 ↔ P1369^{vw}	
	L1074 ↔ F1366^{vw}	L1074 ↔ K1365^{vw}	R1076 ↔ S1309^{vw}	
	E1093 ↔ S1309^{vw}	E1093 ↔ P1369^{vw}	E1093 ↔ H1051^{vw}	
	S1095 ↔ E1368^{vw}			
$x, y, z \leftrightarrow x-1, y, z$	R571 ↔ P1273^{vw}	R571 ↔ P273^{vw}	M576 ↔ P273^{vw}	$2 \times 730\,\text{Å}^2$
$x+1, y, z \leftrightarrow x, y, z$	M576 ↔ P1273^{vw}	M576 ↔ E1252^{vw}	R579 ↔ E1161^{i}	
	R579 ↔ R1256^{i}	E1567 ↔ R1263^{i}	R1571 ↔ R1160^{i}	
	M1576 ↔ R1256^{vw}	M1576 ↔ I1272^{vw}		

[a] Amino acid residues taking part to lattice interactions are indicated in one letter code. They develop hydrogen bonds (^{h}), ionic (^{i}) or Van der Waals (^{vw}) interactions.

[b] For symmetry reasons, each type of contact is found twice (packing valence is 6); the total buried surface is $7040\,\text{Å}^2$.

For numbering of amino acids, see Fig. 2.

Van der Waals type. Expressed in terms of surfaces, the hydrophobic part of the contact areas represents 26.3% in the orthorhombic lattice and 32.5% in the monoclinic lattice. These percentages are significantly greater then the average-accessible hydrophobic surface in free AspRS-1, which is only 12.7% of the total protein surface, indicating that hydrophobic regions are embedded in the crystals during crystallization in both space groups. This surface property of AspRS-1 has to be compared with what found for an average protein where $\sim 55\%$ of the accessible surface is covered by hydrophobic residues [28].

Attractive ionic interactions also participate in packing, but are fewer in number than the hydrophobic interactions. Contacts by hydrogen bonds are even more scarce. The distribution of the charged residues making the salt-bridges is not homogeneous on the protein surface. In monoclinic crystals, 8 out of the 14 salt-bridges are found between dimers related by a crystallographic 2_1 screw axis. In the orthorhombic lattice, 6 out of the 12 residues involved in salt-bridges in one dimer form a cluster with 6 charged residues of another dimer, both dimers being related by the crystallographic 2_1 screw axis parallel to the *a* axis. Two intermolecular hydrogen bonds are found in orthorhombic crystals, but not in monoclinic crystals. Noticeable, in both lattices several close contacts occur between amino acids of the same charge (e.g. E433 ↔ E1336 in monoclinic crystals and R331 ↔ R1353 in orthorhombic crystals). Whether these amino acid proximities mediate binding of cations or anions between neighboring AspRS-1 molecules or represent repulsive zones in larger contact areas is not yet known.

Almost all residues participating in crystal contacts in one crystal form are different from those involved in the other crystal form. In other words, intermolecular contacts are different in the two lattices, and out of the 134 contact residues,

Table 4
Molecular contacts in the monoclinic packing

Contacts between dimers	Residues in interaction[a]			Buried surface[b]
$x, y, z \leftrightarrow -x, -1/2+y, -z$	R312 ↔ E1434^{vw}	R331 ↔ P190^{vw}	A335 ↔ E189^{vw}	2×900 Å^2
$-x, 1/2+y, -z \leftrightarrow x, y, z$	E339 ↔ E1553^{i}	K342 ↔ D1226^{i}	R343 ↔ E1553^{i}	
	W431 ↔ E1336^{vw}	W431 ↔ R1406^{vw}	E433 ↔ E1336^{i}	
	E433 ↔ R1406^{i}	E436 ↔ K1332^{i}	E436 ↔ E1333^{i}	
	E436 ↔ R1406^{i}	E436 ↔ L1410^{vw}	A437 ↔ K1332^{vw}	
	W438 ↔ K1332^{vw}	W438 ↔ A1335^{vw}	W438 ↔ E1336^{vw}	
	W438 ↔ E1339^{vw}	W438 ↔ E1336^{vw}	W438 ↔ E1339^{vw}	
	E457 ↔ R1331^{vw}	D459 ↔ R1331^{i}	D459 ↔ E1338^{i}	
	P460 ↔ R1331^{vw}			
$x, y, z \leftrightarrow x-1, y, z$	P1304 ↔ Y1057^{vw}	Q1308 ↔ L1031^{vw}	E1318 ↔ E1061^{i}	2×410 Å^2
$x+1, y, z \leftrightarrow x, y, z$	R1393 ↔ E1061^{i}	E1457 ↔ L453^{vw}	E1457 ↔ P454^{vw}	
	K1458 ↔ P450^{vw}	R1495 ↔ P454^{vw}	R1495 ↔ K458^{i}	
$x, y, z \leftrightarrow -x, -1/2+y, 1-z$	L31 ↔ E1012^{vw}	L31 ↔ T1013^{vw}	L34 ↔ E1012^{vw}	2×420 Å2
$-x, 1/2+y, 1-z \leftrightarrow x, y, z$	L34 ↔ L1077^{vw}	L34 ↔ R1089^{vw}	F36 ↔ R1089^{vw}	
	Q47 ↔ R1089^{h}	H51 ↔ P1081^{vw}	R76 ↔ P1081^{vw}	
	R76 ↔ R1089^{i}	L77 ↔ P1083^{vw}	P79 ↔ R1089^{vw}	
	E91 ↔ R1089^{i}			
$x, y, z \leftrightarrow -x-1, 1/2+y, -z$	E1502 ↔ F1311^{vw}	E1502 ↔ F1366^{vw}	E1503 ↔ K1365^{i}	2×190 Å^2
$-x-1, -1/2+y, -z \leftrightarrow x, y, z$	E1503 ↔ F1366^{vw}	R1505 ↔ R1312^{i}	R1505 ↔ V1312^{vw}	

[a] Amino acid residues taking part to lattice interactions are indicated in one letter code. They develop hydrogen bonds (^{h}), ionic (^{i}) or Van der Waals (^{vw}) interactions.

[b] For symmetry reasons, each type of contact is found twice (packing valence is 8); the total buried surface is 3840 Å^2.

For numbering of amino acids, see Fig. 2.

only 6 (L34/1034, H51/1051, R76/1076, R331, K1365, and F1366) are found in both lattices (Tables 3 and 4). Moreover, the interactions they produce are different (e.g. R331 interact with either P190 or R1353 in the monoclinic and orthorhombic lattices, respectively). This appears reminiscent to what found for other proteins, such as bovine ribonuclease A crystallizing into six different crystal forms, where crystal contacts comprise different surface regions of the protein [29], or to cutinase, where all pairs of interacting surfaces are different in 14 different crystal contexts [30]. The fact that nearly all surface residues of a protein can be involved at least one time in a crystal contact may mean that crystal contacts make use of randomly selected regions of protein surfaces and is in line with the idea that packing contacts are essentially nonspecific [31,32]. This view, however, holds not for AspRS-1, since in both monoclinic and orthorhombic crystal forms, hydrophobic domains are favored for lattice interactions. Similarly, specific contacts were found important in other crystal packing arrangements, as for instance the anticodon ↔ anticodon contacts in yeast tRNA^{Asp} crystals that mimic the interactions between a tRNA and messenger RNA [33,34].

3.7. Comparison with packing of AspRS-70 from yeast

Even if AspRSs from different organisms, and in particular that from yeast, display the same overall structural organization, they pack differently in crystal lattices. The differences are particularly striking when comparing the packing of AspRS-70 from yeast [20] with those of the two crystal forms of AspRS-1 from *T. thermophilus*. While the

buried surface per AspRS molecule is 2680 Å^2 in the tetragonal packing of the yeast enzyme, it is 7040 Å^2 and 3840 Å^2 in the orthorhombic and monoclinic packing of the synthetase from *T. thermophilus*, respectively (Table 5). Normalizing these values with regard to the molecular masses of the proteins, it appears that the total contact surface in the orthorhombic AspRS-1 crystals is 2.2-fold larger than in the tetragonal yeast AspRS crystals; contact surfaces in the monoclinic *T. thermophilus* and tetragonal yeast AspRS crystals are about similar (Table 5). Noticeable, the few contacts made by the yeast enzyme are predominantly made by hydrogen bonds [20], whereas in the case of the thermostable synthetase from *T. thermophilus* more contacts are formed which are mainly of hydrophobic Van der Waals type. These differences are not well understood, but may be related to the mesophilic and thermophilic nature of the two synthetases. For the thermophilic protein it is likely that evolution has retained a rather robust structure compatible with its activity at high temperature. The consequence is an enhanced crystallizability which may be related to its potential to form large interaction areas. Interestingly, the crystal form of AspRS-1 diffracting to highest resolution (Tables 1 and 5) is the one which develops the largest contact areas in the crystalline lattice.

3.8. Perspectives

Much remains to be discovered about the mechanisms driving protein ↔ protein interactions in a crystallization process. Whether they are mostly driven by the chemical nature of the protein surface or triggered by particular solvent conditions remain open questions. To gain insight into these possibilities, our forthcoming goal is to produce variant proteins with mutations at contact positions in the monoclinic and orthorhombic AspRS-1 crystals. Comparing the crystallization of such mutants will allow to evaluate the influence of packing alterations on crystallizability, crystal stability and crystal perfection. Studying the crystallization of native AspRS will enable to analyze poisoning effects by structural analogues of the crystallizing protein. For that, mutations increasing or decreasing hydrophobic contacts, or creating or disrupting ionic interactions, will be

Table 5
Comparison of packing contacts of AspRSs from *Saccharomyces cerevisiae* and *Thermus thermophilus*

AspRSs	Yeast	*T. thermophilus*	
	(Tetragonal)	(Orthorhombic)	(Monoclinic)
Molecular mass (Da) in crystal	112,000[a]	132,000 (1.18[b])	
Surface of dimer (Å^2)	39,930	48,820	
Dimerization surface (Å^2)	4570 (5390[c])	5570	
No. of contact domains (packing valence)	8 (4 × 2)	6	8
Surface of individual contact domains (Å^2)	2 × 520 (615[c])	1770	900
	2 × 520 (615[c])	1770	900
	2 × 150 (175[c])	1020	410
	2 × 150 (175[c])	1020	410
		730	420
		730	420
			190
			190
Buried surface (Å^2)	2680 (1580[c])		3840 (1.2 ×)
Nature of contacts	Mainly H-bonds	7040 (2.2 ×) Mainly hydrophobic	
Resolution	2.3 Å	2.0 Å	2.6 Å

[a] The crystalline yeast enzyme is a truncated form lacking the 70 N-terminal amino acids (AspRS-70) [35].
[b] Normalization factor between the molecular masses of yeast and *T. thermophilus* crystalline AspRSs.
[c] Normalized surfaces in yeast AspRS-70 for direct comparison with surfaces on the thermophilic AspRS.

prepared. It is expected that modifying the charge distribution of the protein surface may induce changes in crystal packing due to the formation or disruption of salt-bridges. Also, increasing the local surface hydrophobicity may favor formation of new packing contacts.

Acknowledgements

We thank the European Molecular Biology Laboratory at the storage ring DESY, Hamburg, for the beam time allocated to this project. This work was supported by the Centre National de la Recherche Scientifique (CNRS), the Centre National d'Etudes Spatiales (CNES), the Ministère de l'Education Nationale, de la Recherche et de la Technologie (MENRT), Université Louis Pasteur, Strasbourg, and the European Commission (BIO4-CT98-0086). C.C. and C.S. benefited from EC fellowships.

References

[1] R. Giegé, J. Drenth, A. Ducruix, A. McPherson, W. Saenger, Prog. Crystal Growth, Charact. 30 (1995) 237.
[2] A.A. Chernov, Acta Crystallogr. A 54 (1998) 859.
[3] A. McPherson, Crystallization of Biological Macromolecules, Cold Spring Harbor Laboratory Press, Cold Spring Harbor, New York, 1998, p. 586.
[4] M. Delarue, A. Poterszman, S. Nikonov, M. Garber, D. Moras, J.-C. Thierry, EMBO J. 13 (1994) 3219.
[5] H.D. Becker, H. Roy, L. Moulinier, M.-H. Mazauvic, G. Keith, D. Kern, Biochemistry 36 (2000) 8785.
[6] H.D. Becker, R. Giegé, D. Kern, Biochemistry 35 (1996) 7447.
[7] A. Ducruix, R. Giegé, Crystallization of Nucleic Acids and Proteins: A Practical Approach, 2nd Edition, The practical approach series, IRL Press, Oxford, 1999, p. 435.
[8] B. Lorber, C. Sauter, M.-C. Robert, B. Capelle, R. Giegé, Acta Crystallogr. D 55 (1999) 1491.
[9] D.-W. Zhu, B. Lorber, C. Sauter, J.D. Ng, P. Bénas, C. LeGrimellec, R. Giegé, Acta Crystallogr. D 57 (2001) 552.
[10] Z. Otwinowski, W. Minor, Methods Enzymol. 276 (1996) 307.
[11] J. Navaza, P. Saludjian, Methods Enzymol. 276 (1997) 581.
[12] A.T. Brünger, P.D. Adams, G.M. Clore, W.L. DeLano, P. Gros, R.W. Grosse-Kunstlev, J.-S. Jiang, J. Kuszewski, M. Nilges, N.S. Pannu, R.J. Read, L.M. Rice, T. Simonson, G.L. Warren, Acta Crystallogr. D 54 (1998) 905.
[13] G. Kleywegt, A. Jones, Methods Enzymol. 277 (1997) 208.
[14] B. Lee, F.M. Richards, J. Mol. Biol. 55 (1971) 379.
[15] P.R. Schimmel, Annu. Rev. Biochem. 56 (1987) 125.
[16] G. Eriani, M. Delarue, O. Poch, J. Gangloff, D. Moras, Nature 347 (1990) 203.
[17] J.J. Perona, M.A. Rould, T.A. Steitz, Biochemistry 32 (1993) 8758.
[18] J. Cavarelli, B. Rees, G. Eriani, M. Ruff, M. Boeglin, J. Gangloff, J.-C. Thierry, D. Moras, EMBO J. 13 (1994) 327.
[19] H.D. Becker, J. Reinbolt, R. Kreutzer, R. Giegé, D. Kern, Biochemistry 36 (1997) 8785.
[20] C. Sauter, B. Lorber, A. Théobald-Dietrich, R. Giegé, J. Crystal Growth 232 (2001) 399.
[21] B. Lorber, C. Sauter, J.D. Ng, D.-W. Zhu, R. Giegé, O. Vidal, M.-C. Robert, B. Capelle, J. Crystal Growth 204 (1999) 357.
[22] C. Sauter, J.D. Ng, B. Lorber, G. Keith, P. Brion, M.W. Hosseini, J.-M. Lehn, R. Giegé, J. Crystal Growth 196 (1999) 365.
[23] J.D. Ng, B. Lorber, R. Giegé, Life and microgravity Spacelab (LMS), final report, NASA, Marshall Space Flight Center, Alabama, 1998, 130.
[24] S.N. Timasheff, Annu. Rev. Biophys. Biomol. Struct. 22 (1993) 67.
[25] R. Giegé, A. McPherson, in: International Tables for Crystrallography., vol. F (Biological Macromolecules, M. Rossmann, E. Arnold (Eds.)), Kluwer Academic Publishers, Dordrecht, 2001, in press.
[26] B.W. Matthews, J. Mol. Biol. 33 (1968) 491.
[27] S. Martinis, P. Plateau, J. Cavarelli, C. Florentz, Biochimie 81 (1999) 683.
[28] S. Miller, J. Janin, A.M. Lesk, C. Chothia, J. Mol. Biol. 196 (1987) 641.
[29] M.-P. Crosio, J. Janin, M. Jullien, J. Mol. Biol. 228 (1992) 243.
[30] C. Jelsch, S. Longhi, C. Cambillau, Proteins: Struct. Func. Genet. 31 (1998) 320.
[31] J. Janin, F. Rodier, Proteins: Struct. Func. Genet. 23 (1996) 580.
[32] J. Janin, Nat. Struct. Biol. 4 (1997) 973.
[33] D. Moras, A.-C. Dock, P. Dumas, E. Westhof, P. Romby, J.-P. Ebel, R. Giegé, Proc. Natl. Acad. Sci. USA. 83 (1986) 932.
[34] D. Moras, M. Bergdoll, J. Crystal Growth 90 (1988) 283.
[35] C. Sauter, B. Lorber, J. Cavarelli, D. Moras, R. Giegé, J. Mol. Biol. 299 (2000) 1313.